Jurnal Riset Veteriner Indonesia
Journal of the Indonesian Veterinary Research
P-ISSN: 2614-0187, E-ISSN:2615-2835
Volume 4 No. 1 (January 2020), pp. 22-35
journal.unhas.ac.id/index.php/jrvi/

Determining Image Opacity in Broiler Respiratory Radiographic Using ImageJ and Ansel Adam's Zone System

Ikhwan Wirahadikesuma[1,2], Koekoeh Santoso[2], Hera Maheshwari[2], Akhiruddin Maddu[3]

[1]Hospital Pharmacy Installation, Ratu Zalecha Hospital, Jln Menteri Empat, Martapura, South Kalimantan Province, Indonesia
[2]Department of Anatomy, Physiology, and Pharmacology, Faculty of Veterinary Medicine, IPB University, Bogor 16680, Indonesia
[3]Department of Physics, Faculty of Mathematics and Natural Sciences, IPB University, Bogor 16680, Indonesia

*Corresponding author: Ikhwan Wirahadikesuma (ikhwanwira@gmail.com)

Abstract

The diagnosis of diseases of the respiratory, lung, and air sacs generally uses radiographic images by radiologists. Therefore, the results are very subjective, causing differences in the interpretation and diagnosis among different radiologists. A radiographic image reading needs to be made in the form of a simple, fast, and accurate algorithm. The study aimed to reduce subjectivity and be easily carried out by radiology medical personnel, especially veterinarians. This study carried out density measurements by image processing using ImageJ software on 14 radiographic images of broiler chickens. Furthermore, the density value is associated with the Ansel Adam's - grayscale system to determine the opacity of respiratory tract tissues/organs, which were previously inhaled by one of them with chitosan-iopamidol nanoparticles using a nebulizer. The results of density measurements for the category of opacity in radiographic images are that seven spot areas lead brighter (radiopaque) only in chickens that are inhaled mist maker of chitosan-iopamidol nanoparticles. Then the determination of the value range is obtained average value on two ventrodorsal radiographic images, which are inhaled by mist maker of chitosan-iopamidol nanoparticles and chitosan nanoparticle compressor. The conclusion of this study was only in chickens that were infested with mist maker chitosan-iopamidol, whose radiographic image had a radiopaque spot and middle-value area.

Keywords: Ansel Adam's, ImageJ, radiology, radioopaque, subjectivity

Introduction

The respiratory system of poultry has the main functions of oxygen exchange, thermoregulation, and vocalization. Respiratory tract in poultry/chicken starts from nares (nostril) nasal cavities, and there are conchae, then goes to the larynx. The trachea has cartilage rings, syringes until the two-pronged primary extrapulmonary bronchi at the end. Then, the primary extrapulmonary bronchi were followed by the primary intrapulmonary bronchi along the lungs/mesobronchus. The intrapulmonary primary bronchi each go to

the lungs that are connected with the air sacs. The primary bronchi then divide further into the secondary bronchi (consisting of four kinds in the form of mediodorsal, medioventral, lateroventral, laterodorsal) to the parabronchi (tertiary bronchus) either paleopulmonic or neopulmonic. Nine air sacs are consisting of one interclavicular, two cervicals, two cranial thoracics, and two caudal thoracics, and two abdominal (Schmidt and Wild 2014; Powell 2015; Maina 2016). Therefore, it is challenging to extrapolate personal data of chicken respiratory systems as there are different characteristics. It is caused by air sacs and airflow patterns that are bidirectionally and directionally in the parabronchus (Corbine *et al.* 2005; Powell 2015; Dorgan and Takici 2018).

Inhalation therapy uses aerosols with a nebulizer, used for drugs that are given locally to the lungs to get immediate effects, with smaller doses than oral administration (Ikawati 2011). Inhalation therapy is also suitable for animals that experience difficulty in breathing due to respiratory tract disorders (Tell *et al.* 2012). The nanoparticle formulation on iodinate contrast media will provide a longer time in blood circulation, low toxicity, and more importantly can increase the capacity of attenuation (attenuation) of x-rays so that the opacity of imaging results on radiography is better (Shilo *et al.* 2012; Vega and Hafeli 2015).

The diagnosis of lung diseases in poultry is carried out by radiological examination using X-rays by veterinarians. Nowadays, the diagnosis still relies on visual observations and experience in reading radiographic images. So the subjectivity still influences the results of reading/interpreting different radiographic images both at inter and intra-observer (Watiningsih 2012; Listyalina 2017; Sumantri *et al.* 2017). Xavier-Souza *et al.* (2012), in his research on Variation of Chest Radiograph Reading, said that there was disagreement (difference) interpretation of 26 of 803 radiographs conducted by two radiologists (inter-observer).

Ansel Adam's zone system defines a grayscale dividing tonal gradation into eleven discrete zones. Zone V is the middle gray, for textures in an image spanning zones II to VIII. Zone system from 0 to X, wherein zone 0 is maximum black, and zone X is totally white, which can be achieved in photo paper printing or digital forms. For zone IV, it is darker than middle gray (zone V), so are zone III, II, I, and 0, with darker tonal likewise, if white exposure increases one by one from zone V, which is found in zones VI, VII, VIII, IX, and X (Adams and Baker 2005; Lin *et al.* 2012).

Image processing using ImageJ software can be used to determine the density value of lungs and air sacs in radiographic images. Density is a degree of radiographic blackness where higher density values show radiopaque features (Fitriandari et al. 2018). Radiographic images of broiler respiratory tract with black and white images have a degree of gray (grayscale) that can be related to the density of the object. The reading of radiographic images using the Ansel Adam's integrated grayscale system (Ansel Adam's - grayscale) will result in an objective interpretation. To minimize the difference between intra-observer and inter-observer. Image processing on chest radiography can help distinguish between healthy (standard) and unhealthy lungs (Watiningsih 2012; Listyalina 2017; Sumantri *et al.* 2017).

Based on the reasons above, no method has been developed in the form of a simple, fast, and accurate algorithm to reduce the subjectivity of practitioners' interpretation in the field of radiology to analyze radiographic images (chicken respiratory tract). The use of ImageJ software combined with the Ansel Adam's - grayscale zone system can be objective in the form of unchanging and agreed-upon results, even though several practitioners observe a

radiographic image. The study aimed to facilitate medical personnel (practitioners in the field of radiology) to interpret radiographic images in determining opacity in the tissues or organs of the respiratory tract (broiler chickens) based on densities with certain gray levels. So that it can help get the results of interpretation (diagnosis) that is objective, precise, and consistent on radiographic images.

Meterials and Methods

Orientation in determining the dose of contrast media

The determination of iopamidol media contrast dose to be used in broilers begins with dose orientation, which produces radiolucent radiographic images. To inhale the chicken using two doses diluted from the initial preparation, iopamidol concentration of 30.62 gr / 50ml (Iopamiro 300) each dilution dose ten times and 20 times. Then after inhalation, a radiographic image is seen, and a dilution dose of 20 times is chosen because the image results are darker (radiolucent). This dose is then used in the preparation of chitosan-iopamidol nanoparticles. The dose is also used in the inhalation test as a positive control. The dose is the same as the iopamidol concentration of 30.6 mg/ml.

Interpretation of radiographic images

Competent veterinarians were chosen to determine the opacity of radiographic images of broiler respiratory tracts interprets the roentgen results in the form of radiographic images. The results can be radiolucent and radiopaque.

Image processing of radiographic images

This research was conducted using 14 radiographic images of both lateral and ventrodorsal positions. The data in the JPEG format file results from imaging seven male broiler chickens aged two weeks. The radiographs were captured using a roentgen tool with a process duration of about 3 minutes at the Animal Teaching Hospital of Faculty of Veterinary Medicine, IPB University. The Animal Ethics Commission of IPB University approved the study with the number: 147 - 2019. Image processing (Figure 1) is carried out in four stages: radiographic image acquisition, pre-processing (location determination or spot area), radiographic image analysis (density measurement) in the form of radiodensity determination, and percentage of grayscale or opacity percentage for each position.

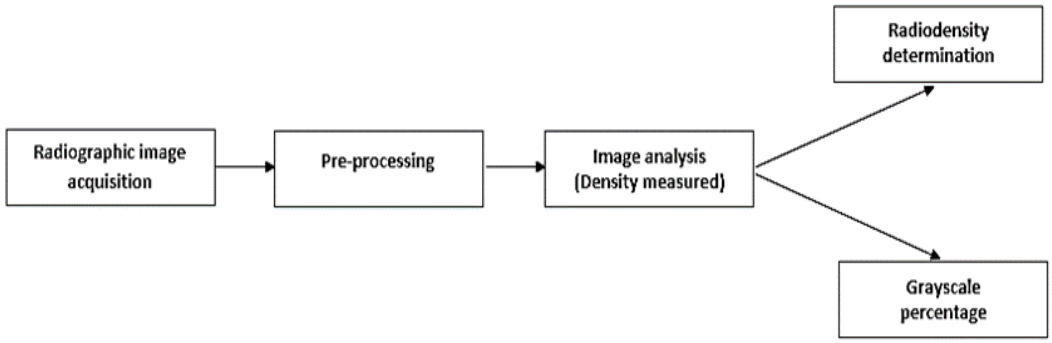

Figure 1. Stages of image processing of radiographic images

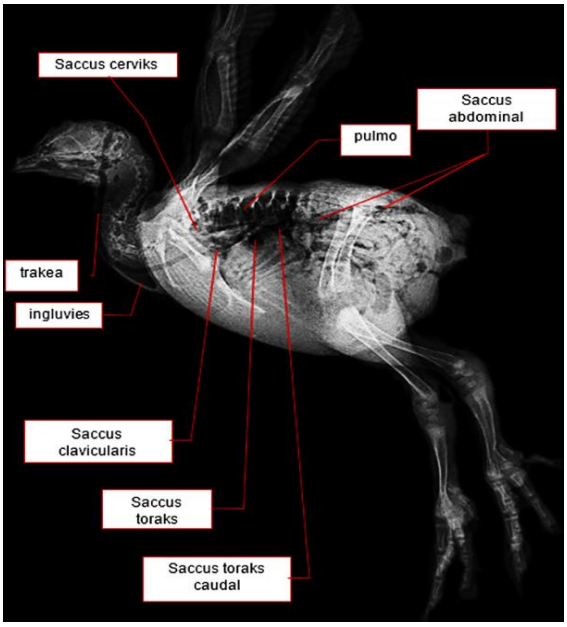

Figure 2. Determination of spot area on lateral position radiography for density measurement

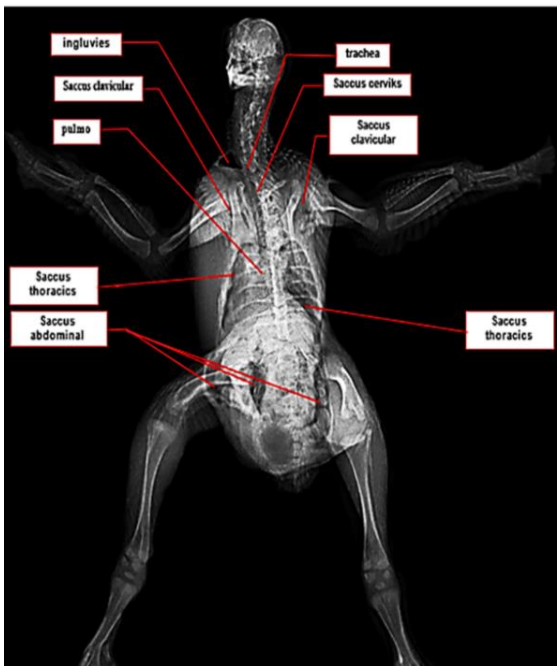

Figure 3. Determination of spot area on radiographs of ventrodorsal position for density measurement

Measurement of spot area density values

Measurement of the density value of the specified spot area on a radiographic image, processed using a computer with ImageJ software (Figure 4). Measurement of density with an area determined using the area selection tools (toolbar) on rectangular selections and menu bars on Analyze and then selecting a measurement shows the density results in mm^2. Measurements are limited to organs in the respiratory system of chickens, namely the lungs and air sacs (saccus pneumatics). Measurement of density values is obtained by adjusting

the scale in the form: area, integrated density, and mean gray value. Organ density profile can be known by using the formula of Gavet and Pines (2010), namely:

Density = *Integrated Density* Value – (The value of the area checked x the mean background value)…….. (1)

Determination of spot area of lungs and air sacs from radiographic images of lateral and ventrodorsal positions can be seen in Figures 2 and 3 based on references to Kobienia (2008) and Maina (2016). Then the spot area density is measured using equation (1). All spot areas are determined with the same area of 72 mm^2, and the data obtained are presented in tabular form.

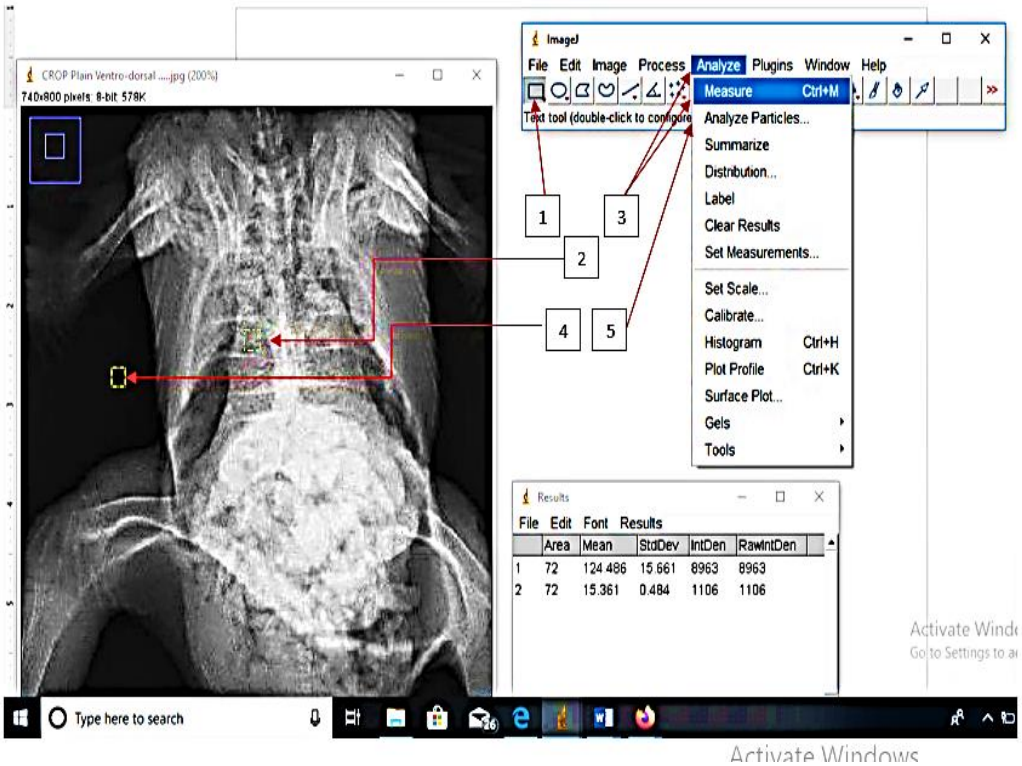

Figure 4. How to measure density using *ImageJ*

The determination of the radiodensity category is based on the Ansel Adam zone system

This image processing analysis is secondary data from radiographic images, the results of radiography (x-ray 30 kVp) in the form of files (softcopy) JPEG format as many as 14 pieces. Determination of the radiodensity of the acquired radiographic image sample, whether it enters the radiopaque or radiolucent category from the spot area whose density value is measured. These values are matched with Table 1, mainly related to the tonal value column. When connected to all density values that are under zone V of the Ansel Adam's system or below 127 grayscale can be categorized as radiolucent and vice versa if above zone V or 127, then radiopaque categories are categorized.

Table 1 Histogram of Ansel Adam's zone system for radiographic image opacity

Zone	0	I	II	III	IV	V	VI	VII	VIII	IX	X
											
Tonal value	0	26	51	77	102	128	153	179	204	230	255
Exposure units	1/2	1	2	4	8	16	32	64	128	256	512
Percent lightness	0	10	20	30	40	50	60	70	80	90	100
Tonal range	0 | 23	24 | 46	47 | 69	70 | 92	93 | 115	116 | 139	140 | 162	163 | 185	186 | 208	209 | 231	232 | 255
	Radiolucent ◄									►	Radiopaque

Source: Lin *et al.* 2012

Table 2 Description of Ansel Adam's zone division

Value Range	Zone	Description
Low Values	0	Total black in print. No useful density in the contrary other than film base-plus-fog.
	I	Effective threshold. The first step above complete black in print, with slight tonality but no texture.
	II	The first suggestion of texture. Deep tonalities, representing the darkest part of the image in which some slight detail is required.
	III	Average dark materials and low values are showing adequate texture.
Middle Values	IV	Average dark foliage, dark stone, or landscape shadow. Average shadow value for Caucasian skin portraits in sunlight.
	V	Middle gray (18% reflectance). The clear north sky as rendered by the panchromatic film, dark skin, gray stone, average weathered wood.
	VI	Average Caucasian skin value in sunlight, diffuse skylight, or artificial light. Light stone, shadows on the snow in sunlit landscapes , clear north sky on panchromatic film with light blue filter.
	VII	Very light skin, light gray objects; average snow with acute side lighting.
	VIII	Whites with texture and delicate values; textured snow; highlights on Caucasian skin.
High Values	IX	White without texture approaching pure white, thus comparable to Zone I in its slight tonality without exact texture. Snow in flat sunlight. With small-format negatives printed with a condenser enlarger, Zone IX may print as pure white not distinguishable from Zone X.
	X	The pure white of the printing paper base; specular glare or light sources in the picture area.

Source: Lin *et al.* 2012

Calculation of opacity percentage on radiographic images

Quantitative determination of radiographic images is by changing the density value to a percentage of gray scales, the density value of each location divided by 255 which is the maximum gray or white scale (Yosimura *et al.* 2011), then multiplied by 100 percent. The calculations are as follows:

Percentage of gray scales = (value of the density of each location/255)x100%..... (2)

Quantitative assessment of equation (2) to see the percentage of opacity or the percentage of brightness (percent lightness) of radiographic images in the lung organs and chicken air sacs, then refer to the calculation pattern of Al Fotawae et al. (2014), with the following equation:

ΣQS = {% Grade anterior + % Grade middle + % Grade posterior}/3..... (3)

Calculation of the percentage of radiographic image opacity is carried out at two exposure positions, namely lateral and ventrodorsal. Each exposition position of all points/locations of the selected spot area is calculated both anteriorly and posteriorly. It is because the respiratory tract of chickens is divided into two parts, namely upper and lower. While in the air sacs also divided into two groups consisting of cranial/front (2 cervical air sacs, one clavicular air sac, two cranial thoracic air sacs) and caudal / back (2 caudal thoracic air sacs, two abdominal air sacs) (Powell 2015). So it is quite difficult to determine each air sac on radiographs that are acquired, because some have no clear boundaries and cover each other, especially on lateral position radiographic exposures. For this reason, the average percentage of opacity calculation is as follows:

ΣQS = {Total number of gray scales in each exposition position (x)} / {total number of locations (n)}..... (4)

The quantitative value of each radiographic image obtained can be linked to the Ansel Adam's zone in Table 2, and Table 3 to determine the value range categories, as well as the results in tabular form.

Data Analysis

Qualitative analysis was carried out by a competent veterinarian to determine the opacity of the broiler chicken respiratory tract. For quantitative analysis, radiographic images that are acquired in the JPEG format as data are processed using ImageJ software. The density measurement is then linked to the Ansel Adam's zone system, which is integrated with the grayscale (Ansel Adam's-gray scale) to determine the radiolucent and radiopaque. The results are described in tabular form.

Results and Discussion

The characteristics of contrast media (chitosan-iopamidol nanoparticle formulation)

Earlier in the respiratory tract of broiler chickens carried out x-ray scanning with the results in the form of radiography, then interpreted by a veterinarian visually as a radiological practitioner. Previously the chicken was inhaled with two types of nebulizer, namely mist maker for 6.5 minutes and 13 minutes compressor. Inhalation was given when the chicken inspires. The aerosols also carry the flow of gas into the respiratory tract. Aerosols used are of three kinds of solutions, namely: chitosan nanoparticle solution, chitosan-iopamidol nanoparticle solution, and iopamidol solution concentration of 30.6 mg/ml. The results of the interpretation of inhaled chickens with chitosan-iopamidol nanoparticle solution, which, when preparation/synthesis using iopamidol concentration of 30.6 mg/ml, can still provide excellent x-ray imaging (Wirahadikesuma *et al.* 2019).

Chitosan-iopamidol nanoparticle solution synthesized by the ionic gelation method, the characteristics of the dosage form appear oplacent, the particle size is 409.3 nm, the polydispersity index is 0.53 showing good and homogeneous size uniformity so that deposits and aggregates are also formed very little. The Fourier Tansform Infrared Spectroscopy (FTIR) spectra showed an absorption band with a peak of 3237 cm-1 indicating that it was related to the bonding of hydrogen molecules from the combining of chitosan with Sodium triphosphate (Na-TPP) and having a morphology that tends to be round (Figure 5) (Wirahadikesuma *et al.* 2019).

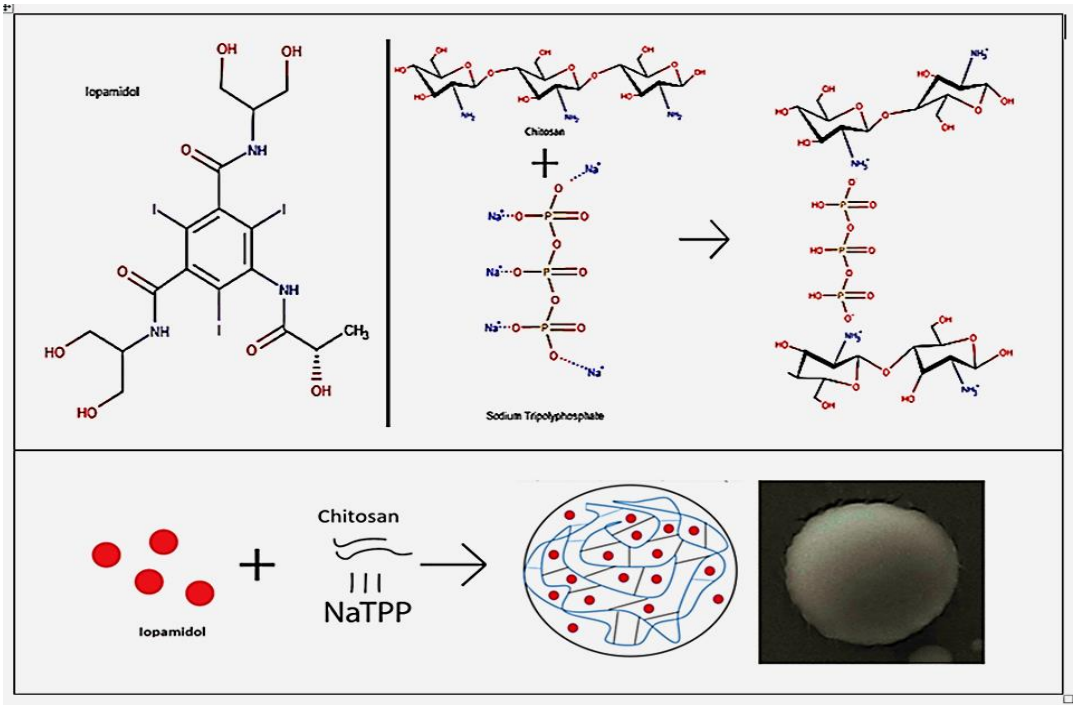

Figure 5. The chemical structure of iopamidol molecules and the process of chitosan crosslinking with sodium tripolyphosphate

Image processing radiographic images of lung organs and air sacs

The examination of radiographs was carried out visually by observing images directly by medical personnel, requiring concentration and accuracy. To handle these problems, image processing can be used to process data into information. The data is in the form of radiographic images that are processed so that the information obtained is better and objective. It is expected to help determine the opacity in detecting the patient's status (chicken as a patient) on radiographic images so that it is known whether tissue or organ is disturbed or not.

The results of radiographic image processing on density measurements using ImageJ software and the determination of the radiodensity category using the Ansel Adam's zone system approach can be seen in Table 3. The results obtained are expected to help reduce the subjectivity of practitioners' interpretation so that they become objective. It is because each spot area in a radiographic image has its density measured using ImageJ to produce a value. In contrast, the results of subjective visual observation are strongly influenced by experience. Then the density values obtained are matched into the Ansel Adam's - grayscale system to determine each spot area, whether it is more towards white/bright or black/dark. A spot area is categorized as radiopaque (radiopaque) if it is located in the Ansel Adam's-gray scale system zone in zone V and above. Vice versa, for the spot area under zone V,

categorized radiolucent (radiolucent). In zone V in Ansel Adam's system, it has a density of 127/128, which is the average value of the chosen figure 127 or 128 as mid-gray (middle gray) in the grayscale range of 0-255. Values below or above the mid-gray value indicate that images tend to be dark or bright (Dougherty 2009). Middle gray itself in the Ansel Adam's system zone with a value of 128 on the tonal histogram value (Table 1). Middle gray is equivalent to a reflectance of 18% of the right gray value in the middle of a geometric scale from black to white (Lin et al. 2012).

Radiopaque or radiolucent at each spot area on the radiographic image represents the amount of radiodensity in the tissue structure through which x-rays travel. The composition of human and animal tissues is divided into four main radiodensity categories, and two substances are often used for diagnosis in therapy. The anatomical/radiodensity identification in the body is based on radiographic contrast in radiographic images from the least radiodense (radiolucent) to the most radiodense (radiopaque), which consists of air, fat, water, bone, contrast media and heavy metals. The term radiodense is used instead to describe areas where radiodensity is increasing (McKinnis 2010).

Table 3. The radiographic density values obtained are related to the radiodensity category based on Ansel Adam's zone

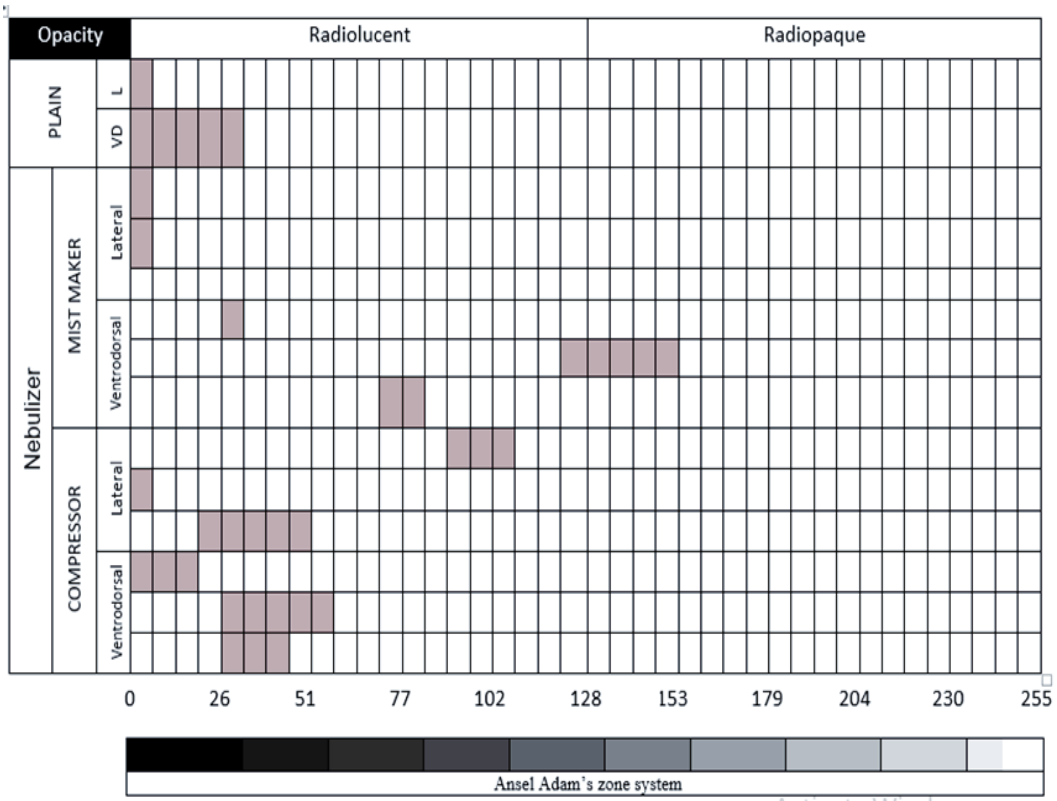

Note: L = Lateral; VD = Ventrodorsal

The contrast media used in this study was chitosan-iopamidol nanoparticles (formula B) and iopamidol concentrations of 30.6 mg/ml (formula C) every 1 ml equivalent to 1/20 dose intravenous Computerized Tomography Scan (CT Scan) in humans. Table 3 and Figure 6 the attenuation power of contrast media, which gives radiopaque only to the radiographic images of chitosan-iopamidol nanoparticle positions in 7 ventrodorsal positions in the spot area. The density values for each of these spot areas are: 1 = 151.31; 2 = 131.74; 3 = 138.25; 4 = 147.62; 5 = 137.29, and 8 = 148.66. All seven-spot area values are above the middle gray density value (128) or more towards the light zone or radiopaque. So that in interpreting radiographic images with image processing that is

connected to the Ansel Adam's - grayscale zone system, it is obtained in the form of an algorithm to determine its opacity and categories, as can be seen in Figure 7.

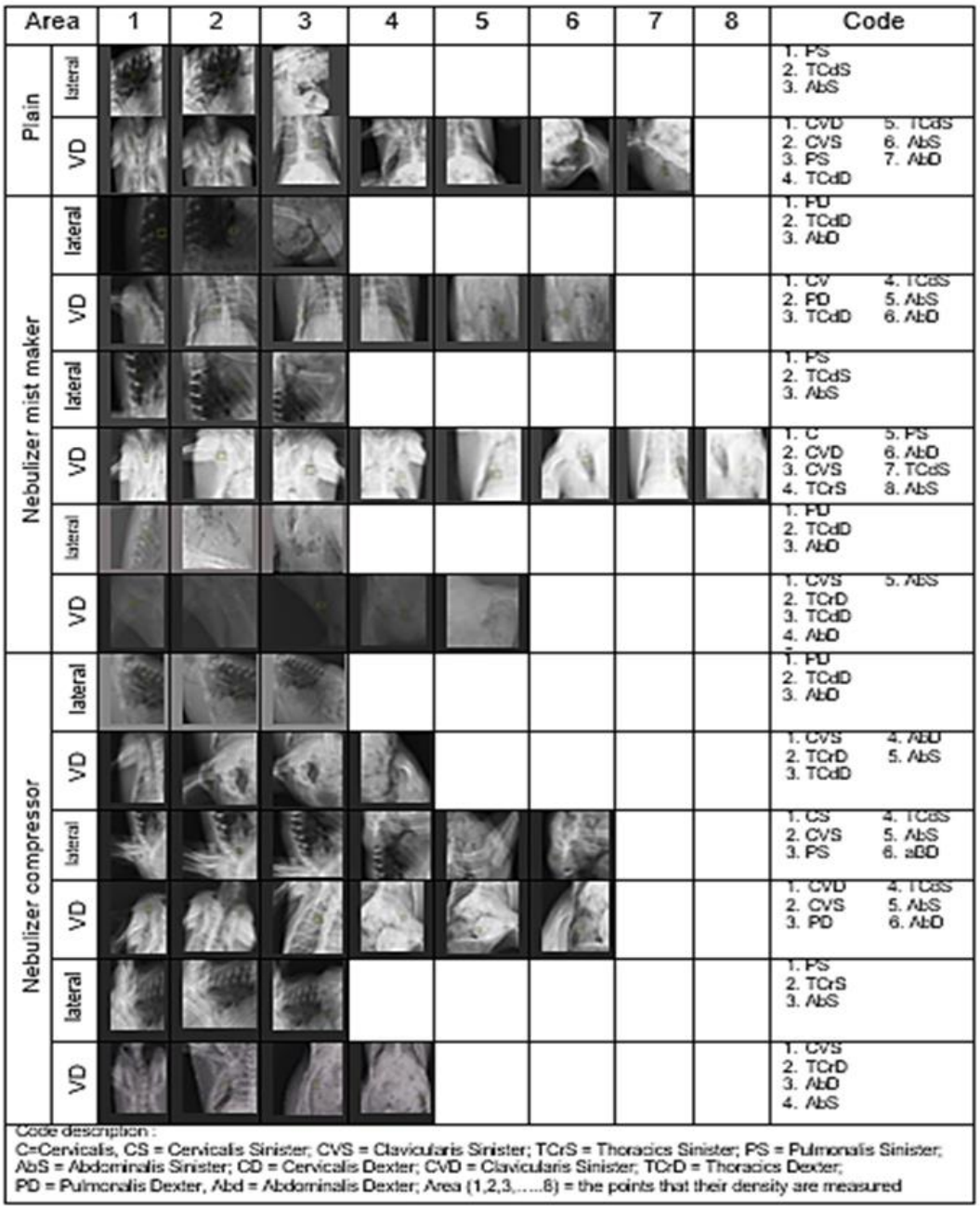

Figure 6. Pieces of radiographic images of each spot area in the lateral and ventrodorsal positions

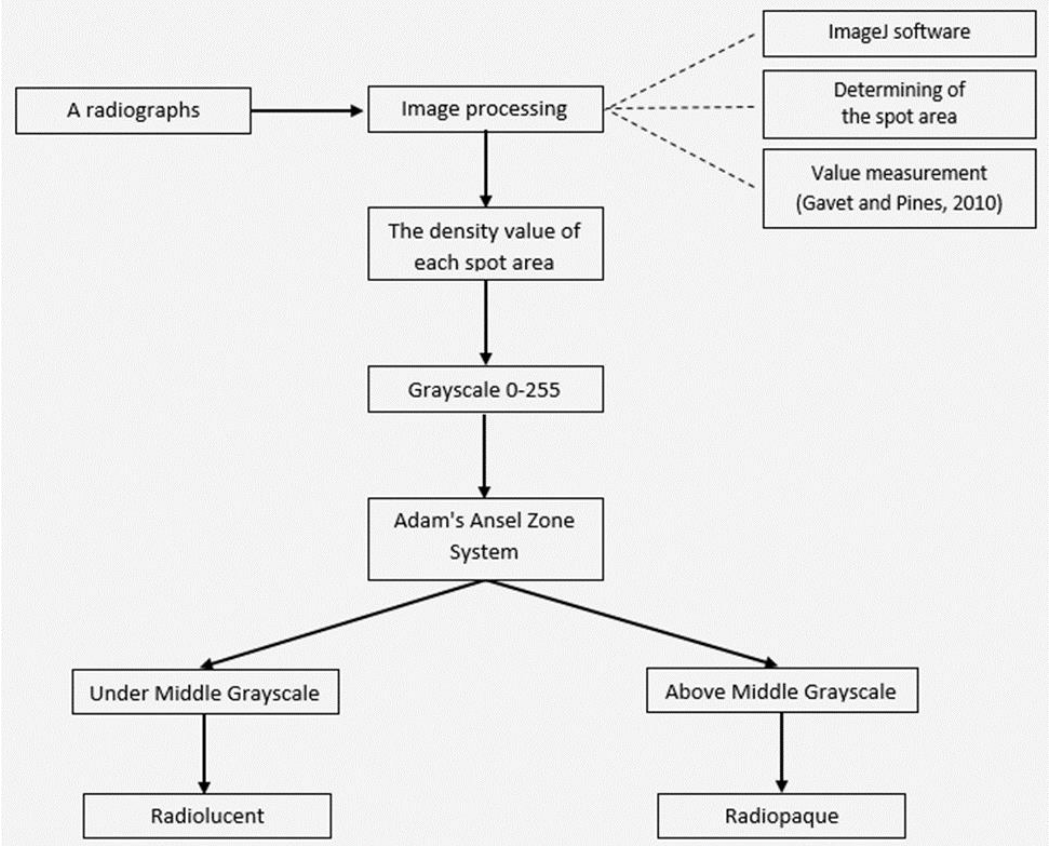

Figure 7. Algorithm of the stages of determining opacity (radiodensity category) of radiographic images

Percentage of opacity in radiographic images

Determination of the value range on a sheet of radiographic image files from a collection of several spot areas gives an illustration that the observation / reading area can be classified as low value, average value, and high value. The histogram is divided equally into 11 areas to represent the zone system to show relative brightness, which is shown in Table 1. Meanwhile, matching 0-256 (grayscale) tonal values into eleven zones by applying brightness percentages for each zone, zone 0 is 0 % sunny, then the next zone goes up 10% up to zone X, which is 100% sunny.

Table 4 showed that the value range based on Ansel Adam's zone (Tables 1 and 2) on radiographic images of two types of nebulizers with three different solution formulas. For the mist maker nebulizer formula B, the ventrodorsal position is the percentage of opacity obtained in the average value (around middle gray) while the compressor nebulizer is in the lateral position A formula — all equations using water solvents (aquabidestillata and aquademineralisata), which have radiodensity over fat and air. On the radiographic area of the ventrodorsal radiodensity into the middle zone, the possibility of aerosol formula B from the nebulizer mist maker and formula A from the compressor nebulizer is more in the air, resulting in aerosol density and thickness in the respiratory tract of chickens, increasing the attenuation especially in the air sacs (lumen) filled with contrast media. Radiodensity, in addition to tissue composition, is also determined by the thickness (density) of an object, the thicker an object. The more radiodensity that is possessed relative to objects thinner than the same material, thus causing weakening of x-rays after passing through objects or objects and increasing the density of radiographic images (McKinnis 2010).

Table 4. Average percentage of opacity (percent lightness) of lateral and ventrodorsal positions on radiographic images

Type of inhalation formula	Position of X-ray	percentage of opacity (nebulizer mist maker)	Value range	percentage of opacity (nebulizer compressor)	percentage of opacity (without nebulizer)	Value range
(P). Plain (without formula solution)	lateral				2.64	Low value
	ventrodorsal				7.36	Low value
(A). Nanoparticles of Chitosan (without iopamidol)	lateral	2.94	Low value	39.40		Middle value
	ventrodorsal	12.68	Low value	6.59		Low value
(B). Nanoparticles of Chitosan-iopamidol	lateral	3.11	Low value	5,00		Low value
	ventrodorsal	54.54	Middle value	22.64		Low value
(C). Iopamidol 30,6 mg/ml	lateral	0	-	11.28		Low value
	ventrodorsal	7.01	Low value	13.47		Low value

Conclusion

From this study, it can be concluded that:

1. The results of determining the category of opacity only on radiographic images inhaled by mist maker nebulizer, nanoparticles of chitosan-iopamidol ventrodorsal position visible radiopaque (lighter) above the middle gray of 7 spot areas.
2. The digital sheet image of chitosan nanoparticle radiographs (compressor nebulizer) and contrast media chitosan-iopamidol naoparticles (mist maker nebulizer) can provide opacity in the respiratory tract of broiler chickens with a percentage of opacity = middle value.
3. Image processing algorithm with imageJ combined with Ansel Adam's zone system - gray scale can be used to determine radiographic / opacity radiographic images of broiler respiratory tracts.

Acknowledgment

The authors would like to thank the Banjar District Government of South Kalimantan for granting a study permit. The authors thank Mokhamad Fahrul Ulum for his input and Muhamad Risman Wahid for his assistance.

Reference

Adams A, Baker R., 2005. *Zone System (Photography) in The Negative*. The Ansel Adams Photography Series Book 2; p. 47-97. Little, Brown and Company, New York

Al-Fotawei R, Ayoub AF, Heath N, Naudi KB, Tanner KE, Dalby MJ, Mc Mahon J., 2014. Radiological Assessment of BioengineeredCorbanie EA, Matthijs MGR, Van Eck JHH, Remon JP, Landman WJM, Vervaet C. 2006. Deposition of differently sized airborne microspheres in the respiratory tract of chickens, *Avian Pathology*. (35-6); p. 475–485. DOI: 10.1080/03079450601028845

Dogan GK, Takici I., 2018. Anatomy of Respiratory System in Poultry, *MAE Vet Fak Derg*, 3 (2); p. 141-147, DOI: 10.24880/maeuvfd.433946.

Dougherty G., 2009. *Digital Image Processing for Medical Applications*, Cambridge University Press, The Edinburgh Building, Cambridge CB2 8RU. United Kingdom; p. 137-139.

Fitriandari BQ, Pramanik F, Farah RA., 2018. Gambaran Proses Penyembuhan Lesi Periapikal pada Radiografi Periapikal Menggunakan Software ImageJ, *Padjadjaran Journal of Dental Researchers and Students*. vol. 2 (1); p 116-122

Gavet OP, Pines J., 2010. Progressive Activation of CyclinB1-Cdk1 Coordinates Entry to Mitosis. *Developmental Cell.* vol. 18 (4); p. 533-543. Elsevier

Ikawati Z., 2011. *Penyakit Sistem Pernapasan dan Tata Laksana Terapinya*. Yogyakarta: Bursa Ilmu; p. 263-275.

Kobienia VM., 2008. *Schnittbildanatomie des Haushuhnes (Gallus domesticus) anhand von sekundären Scheibenplastinaten, Sectional anatomy of the domestic fowl (Gallus domesticus) using the secondary sheet plastinates*, the Veterinary Faculty of the Ludwig-Maximilians University of Munich/München; p. 19-47

Lin JS, Liao YY, Tai SC, 2012. Color Correction with Zone System for Color Image, *International Journal of Digital Content Technology and its Applications* (JDCTA), vol. 6 (10); p. 257-265 doi:10.4156/jdcta.vol6.issue10.30

Listyalina, L., 2017. Peningkatan Kualitas Citra Foto Rontgen Sebagai Media Deteksi Kanker Paru, *Jurnal Teknologi Informasi*, vol. XII (34); p. 100-118.

Maina JN., 2008. Functional morphology of the avian respiratory system, the lung–air sac system: efficiency built on complexity. *Ostrich*, vol. 79 (2); p. 117–132. doi:10.2989/ostrich.2008.79.2.1.575

Maina JN. 2016. Pivotal debates and controversies on the structure and function of the avian respiratory system: setting the record straight*. Biological Reviews,* vol*.* 92(3); p 1475–1504.doi:10.1111/brv.12292

McKinnis LN., 2010. *Fundamentals of musculoskeletal imaging*, 3rd edition, ISBN 978-0-8036-1946-3 1, F.A.Davis Company 1915 Arch Street, Philadelphia, PA 19103; p. 10-13.

Powell FL., 2015., *Respiration.* Chapter-13, Sturkie's Avian Physiology, Editor Colin G. Scanes, Six Edition. USA: Academic Press, Elsevier; p. 301-307doi:10.1016/b978-0-12-407160-5.00013-0

Schmidt MF, Wild M., 2014. The Respiratory Vocal System of Songbirds: Anatomy, Physiology, and Neural Control. *Progress in Brain Research*, vol. 212; p 297-335. Elsevier. https://doi.org/10.1016/B978-0-444-63488-7.00015-X

Shilo M, Reuveni T, Motiei, M, Popovtzer R., 2012. Nanoparticles as computed tomography contrast agents: current status and future perspectives. *Nanomedicine*. vol 7 (2); p 257-269.

Sumantri DDS, Firman RN, Azhari A., 2017. Analisis radiografi periapikal menggunakan software imageJ pada abses periapikal setelah perawatan endodontik. *Majalah Kedokteran Gigi Indonesia*, vol. 3(1); p. 29-34.

Tell LA, Stephens K, Teague SV, Pinkerton KE, Raabe OG., 2012. Study of Nebulization Delivery of Aerosolized Fluorescent Microspheres to The Avian Respiratory Tract. HHS Public Access. : *Avian Dis*, vol. 56 (2); p. 381–386

Vega JCDL, Häfeli UO., 2015. Utilization of nanoparticles as X-ray contrast agents for diagnostic imaging applications. *Contrast Media Mol. Imaging*, vol. 10 (2); p. 81 – 95

Watiningsih T., 2012. Pengolahan Citra Foto Sinar-X Untuk Mendeteksi Kelainan Paru. *Teodolita,* vol.13 (1); p. 14-30.

Wirahadikesuma I, Santoso K, Maheshwari H, Maddu A., 2019. Efektivitas Pemberian Nanopartikel Kitosan-Iopamidol Menggunakan Nebulizer Pada Saluran

Pernapasan Ayam Broiler Berdasarkan Hasil Pencitraan Sinar-x. JCPS (*Journal of Current Pharmaceutical Sciences*), vol. 3(1); p.198-205

Xavier-Souza G, Vilas-Boas AL, Fontoura MSH, Araújo-Neto CA, Andrade SC, Cardoso, MRA, ... & PNEUMOPAC-Efficacy Study Group., 2013. The inter-observer variation of chest radiograph reading in acute lower respiratory tract infection among children. *Pediatric pulmonology*, vol. 48(5); p. 464-469

Yoshimura K, Shimamoto K, Ikeda M, Ichikawa K, Naganawa, S., 2011*. A Comparative Contrast Perception Phantom Image of Brain CT Study Between High-grade and Low-Grade Liquid Crystal Displays (LCDs) in Electronic Medical Charts. Physica Medica*, vol. 27 (2); p. 109–116. doi:10.1016/j.ejmp.2010.06.001